AdaptDiffuser: Diffusion Models as Adaptive Self-evolving Planners

Zhixuan Liang [1] **Yao Mu** [1] **Mingyu Ding** [1 2] **Fei Ni** [3] **Masayoshi Tomizuka** [2] **Ping Luo** [1]

Abstract

Diffusion models have demonstrated their powerful generative capability in many tasks, with great potential to serve as a paradigm for offline reinforcement learning. However, the quality of the diffusion model is limited by the insufficient diversity of training data, which hinders the performance of planning and the generalizability to new tasks. This paper introduces AdaptDiffuser, an evolutionary planning method with diffusion that can self-evolve to improve the diffusion model hence a better planner, not only for seen tasks but can also adapt to unseen tasks. AdaptDiffuser enables the generation of rich synthetic expert data for goal-conditioned tasks using guidance from reward gradients. It then selects high-quality data via a discriminator to finetune the diffusion model, which improves the generalization ability to unseen tasks. Empirical experiments on two benchmark environments and two carefully designed unseen tasks in KUKA industrial robot arm and Maze2D environments demonstrate the effectiveness of AdaptDiffuser. For example, AdaptDiffuser not only outperforms the previous art Diffuser (Janner et al., 2022) by 20.8% on Maze2D and 7.5% on MuJoCo locomotion, but also adapts better to new tasks, e.g., KUKA pick-and-place, by 27.9% without requiring additional expert data.

1. Introduction

Offline reinforcement learning (RL) (Levine et al., 2020; Prudencio et al., 2022) aims to learn policies from previously collected offline data without interacting with the live environment. Traditional offline RL approaches require fitting value functions or computing policy gradients, which are challenging due to limited offline data (Agarwal et al., 2020; Kumar et al., 2020; Wu et al., 2019; Kidambi et al., 2020).

(a) Illustration of AdaptDiffuser.

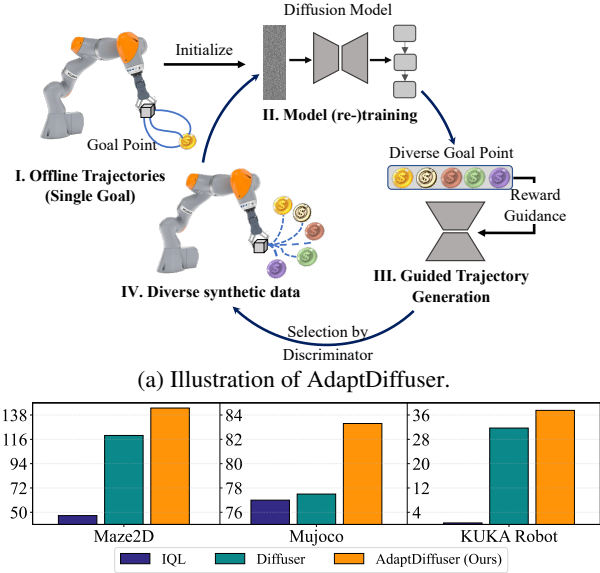(b) Performance comparisons on three benchmarks.

Figure 1. Overall framework and performance comparison of AdaptDiffuser. It enables diffusion models to generate rich synthetic expert data using guidance from reward gradients of either seen or unseen goal-conditioned tasks. Then, it iteratively selects high-quality data via a discriminator to finetune the diffusion model for self-evolving, leading to improved performance on seen tasks and better generalizability to unseen tasks.

Recent advances in generative sequence modeling (Chen et al., 2021a; Janner et al., 2021; 2022) provide effective alternatives to conventional RL problems by modeling the joint distribution of sequences of states, actions, rewards and values. For example, Decision Transformer (Chen et al., 2021a) casts offline RL as a form of conditional sequence modeling, which allows more efficient and stable learning without the need to train policies via traditional RL algorithms like temporal difference learning (Sutton, 1988). By treating RL as a sequence modeling problem, it bypasses the need of bootstrapping for long-term credit assignment, avoiding one of the "deadly triad" (Sutton & Barto, 2018) challenges in reinforcement learning.

To this end, it is essential to devise better sequence modeling algorithms for the new generation of offline RL. The diffusion probability model (Rombach et al., 2022; Ramesh et al., 2022), with its demonstrated success in generative sequence modeling for natural language processing and

[1]Department of Computer Science, The University of Hong Kong, Hong Kong SAR [2]UC Berkeley, USA [3]College of Intelligence and Computing, Tianjin University, Tianjin, China. Correspondence to: Ping Luo <pluo.lhi@gmail.com>.

computer vision, presents an ideal fit for this endeavor. It also shows its potential as a paradigm for planning and decision-making. For example, diffusion-based planning methods (Janner et al., 2022; Ajay et al., 2022; Wang et al., 2022b) train trajectory diffusion models based on offline data and apply flexible constraints on generated trajectories through reward guidance during sampling. In consequence, diffusion planners show notable performance superiority compared with transformer-based planners like Decision Transformer (Chen et al., 2021a) and Trajectory Transformer (Janner et al., 2021) on long horizon tasks, while enabling goal-conditioned rather than reward-maximizing control at the same time.

While diffusion planners have achieved success in certain areas, their performance is limited by the lack of diversity in their training data. In decision-making tasks, the cost of collecting a diverse set of offline training data can be high, and this insufficient diversity would impede the ability of the diffusion model to accurately capture the dynamics of the environment and the behavior policy. As a result, diffusion models tend to perform inferior when expert data is insufficient, or particularly, faced with new tasks. This raises a natural question: can we use the synthetic data generated by the diffusion model to improve the diffusion model itself given its powerful generative sequence modeling capability? Enabling the diffusion model self-evolutionary can make it a stronger planner, potentially benefiting more decision-making requirements and downstream tasks.

In this paper, we present AdaptDiffuser, a diffusion-based planner for goal-conditioned tasks that can generalize to novel settings and scenarios through self-evolution (see Figure 1). Unlike conventional approaches that rely heavily on specific expert data, AdaptDiffuser uses reinforcement learning reward gradients as guidance to generate rich and diverse synthetic demonstration data for both existing and unseen tasks. The generated demonstration data is then filtered by a discriminator, where those high-quality ones are used to fine-tune the diffusion model, resulting in a better planner with significantly improved self-bootstrapping capabilities on previously seen tasks and an enhanced ability to generalize to new tasks. As a consequence, AdaptDiffuser not only improves the performance of the diffusion-based planner on existing benchmarks, but also enables it to adapt to unseen tasks without the need for additional expert data.

It's non-trivial to construct and evaluate AdaptDiffuser for both seen and unseen tasks. We first conduct empirical experiments on two widely-used benchmarks (MuJoCo (Todorov et al., 2012) and Maze2d) of D4RL (Fu et al., 2020) to verify the self-bootstrapping capability of AdaptDiffuser on seen tasks. Additionally, we creatively design new pick-and-place tasks based on previous stacking tasks in the KUKA (Schreiber et al., 2010) industrial robot arm environ-

ment, and introduce novel auxiliary tasks (e.g., collecting gold coins) in Maze2D. The newly proposed tasks and settings provide an effective evaluation of the generalization capabilities of AdaptDiffuser on unseen tasks.

Our contributions are three-fold: **1)** We present AdaptDiffuser, which allows diffusion-based planners to self-evolve for offline RL by generating synthetic expert data with the diffusion model and filtering out high-quality examples with the guidance of reward. **2)** We apply our self-evolutionary diffusion-based planner to unseen manipulation tasks without any additional expert data, demonstrating its strong generalization ability. **3)** Extensive experiments on two widely-used offline RL benchmarks from D4RL as well as our carefully designed unseen tasks in KUKA and Maze2d environments validate the effectiveness of AdaptDiffuser.

2. Related Works

Offline Reinforcement Learning. Offline RL (Levine et al., 2020; Prudencio et al., 2022) is a popular research field that aims to learn behaviors using only offline data such as those collected from previous experiments or human demonstrations, without the need to interact with the live environment from time to time at the training stage.

However, in practice, offline RL faces a major challenge that standard off-policy RL methods may fail due to the overestimation of values, caused by the distribution deviation between the offline dataset and the policy to learn. Most conventional offline RL methods use action-space constraints or value pessimism (Buckman et al., 2020) to overcome the challenge (Agarwal et al., 2020; Kumar et al., 2020; Siegel et al., 2020; Wu et al., 2019; Yang et al., 2022). For example, conservative Q-learning (CQL) (Kumar et al., 2020) addresses these limitations by learning a conservative Q-function, ensuring the expected value under this Q-function is lower than its true value.

Reinforcement Learning as Sequence Modeling. Recently, a new paradigm for Reinforcement Learning (RL) has emerged, in which RL is viewed as a generic sequence modeling problem. It utilizes transformer-style models to model trajectories of states, actions, rewards and values, and turns its prediction capability into a policy that leads to high rewards. As a representative, Decision Transformer (DT) (Chen et al., 2021a) leverages a causally masked transformer to predict the optimal action, which is conditional on an autoregressive model that takes the past state, action, and expected return (reward) into account. It allows the model to consider the long-term consequences of its actions when making a decision. And based on DT, Trajectory Transformer (TT) (Janner et al., 2021) is proposed to utilize transformer architecture to model distributions over trajectories, repurposes beam search as a planning al-

gorithm, and shows great flexibility across long-horizon dynamics prediction, imitation learning, goal-conditioned RL, and offline RL. Bootstrapped Transformer (Wang et al., 2022a) further incorporates the idea of bootstrapping and uses the learned model to self-generate more offline data to further improve sequence model training. However, such approaches lack flexibility in adapting to new reward functions or tasks in different environments, as the generated data is not suitable for use in new tasks or environments. Diffuser (Janner et al., 2022) presents a powerful framework for trajectory generation using the diffusion probabilistic model, which allows the application of flexible constraints on generated trajectories through reward guidance during sampling. The consequent work, Decision Diffuser (Ajay et al., 2022) introduces conditional diffusion with reward or constraint guidance for decision-making tasks, further enhancing Diffuser's performance. Additionally, Diffusion-QL (Wang et al., 2022b), adds a regularization term to the training loss of the conditional diffusion model, guiding the model to learn optimal actions. Nevertheless, the performance of these methods is still limited by the quality of offline expert data, leaving room for improvement in adapting to new tasks or settings.

Diffusion Probabilistic Model. Diffusion models are a type of generative model that represents the process of generating data as an iterative denoising procedure (Sohl-Dickstein et al., 2015; Ho et al., 2020). They have made breakthroughs in multiple tasks such as image generation (Song et al., 2021), waveform generation (Chen et al., 2021b), 3D shape generation (Zhou et al., 2021) and text generation (Austin et al., 2021). These models, which learn the latent structure of the dataset by modeling the way in which data points diffuse through the latent space, are closely related to score matching (Hyvärinen, 2005) and energy-based models (EBMs) (LeCun et al., 2006; Du & Mordatch, 2019; Nijkamp et al., 2019; Grathwohl et al., 2020), as the denoising process can be seen as a form of parameterizing the gradients of the data distribution (Song & Ermon, 2019).

Moreover, in the sampling process, diffusion models allow flexible conditioning (Dhariwal & Nichol, 2021) and have the ability to generate compositional behaviors (Du et al., 2020). It shows that diffusion models own promising potential to generate effective behaviors from diverse datasets and plan under different reward functions including those not encountered during training.

3. Preliminary

Reinforcement Learning is generally modeled as a Markov Decision Process (MDP) with a fully observable state space, denoted as $\mathcal{M} = (\mathcal{S}, \mathcal{A}, \mathcal{T}, \mathcal{R}, \gamma)$, where $\mathcal{S}$ is the state space and $\mathcal{A}$ is the action space. Besides, $\mathcal{T}$ is the state transition

function with the dynamics of this discrete-time system that $s_{t+1} = \mathcal{T}(s_t, a_t)$ at state $s_t \in \mathcal{S}$ given the action $a_t \in \mathcal{A}$. $\mathcal{R}(s_t, a_t)$ defines the reward function and $\gamma \in (0, 1]$ is the discount factor for future reward.

Considering the offline reinforcement learning as a sequence modeling task, the objective of trajectory optimization is to find the optimal sequence of actions $a_{0:T}^*$ that maximizes the expected return with planning horizon T, which is the sum of per time-step rewards or costs $R(s_t, a_t)$:

$$a_{0:T}^* = \arg\max_{a_{0:T}} \mathcal{J}(s_0, a_{0:T}) = \arg\max_{a_{0:T}} \sum_{t=0}^{T} \gamma^t R(s_t, a_t). \tag{1}$$

The sequence data generation methods utilizing diffusion probabilistic models (Sohl-Dickstein et al., 2015; Ho et al., 2020) pose the generation process as an iterative denoising procedure, denoted by $p_\theta(\tau^{i-1} \mid \tau^i)$ where τ represents a sequence and i is an indicator of the diffusion timestep.

Then the distribution of sequence data is expanded with the step-wise conditional probabilities of the denoising process,

$$p_\theta\left(\tau^0\right) = \int p\left(\tau^N\right) \prod_{i=1}^{N} p_\theta\left(\tau^{i-1} \mid \tau^i\right) \mathrm{d}\tau^{1:N} \tag{2}$$

where $p\left(\tau^N\right)$ is a standard normal distribution and τ^0 denotes original (noiseless) sequence data.

The parameters θ of the diffusion model are optimized by minimizing the evidence lower bound (ELBO) of negative log-likelihood of $p_\theta\left(\tau^0\right)$, similar to the techniques used in variational Bayesian methods.

$$\theta^* = \arg\min_\theta -\mathbb{E}_{\tau^0}\left[\log p_\theta\left(\tau^0\right)\right] \tag{3}$$

What's more, as the denoising process is the reverse of a forward diffusion process which corrupts input data by gradually adding noise and is typically denoted by $q\left(\tau^i \mid \tau^{i-1}\right)$, the reverse process can be parameterized as Gaussian under the condition that the forward process obeys the normal distribution and the variance is small enough (Feller, 2015).

$$p_\theta\left(\tau^{i-1} \mid \tau^i\right) = \mathcal{N}\left(\tau^{i-1} \mid \mu_\theta\left(\tau^i, i\right), \Sigma^i\right) \tag{4}$$

in which μ_θ and Σ are the mean and covariance of the Gaussian distribution respectively.

For model training, with the basis on Eq. 3 and 4, (Ho et al., 2020) proposes a simplified surrogate loss:

$$\mathcal{L}_{\text{denoise}}(\theta) := \mathbb{E}_{i, \tau^0 \sim q, \epsilon \sim \mathcal{N}}[||\epsilon - \epsilon_\theta(\tau^i, i)||^2] \tag{5}$$

where $i \in \{0, 1, ..., N\}$ is the diffusion timestep, $\epsilon \sim \mathcal{N}(\mathbf{0}, \mathbf{I})$ is the target noise, and τ^i is the trajectory τ^0 corrupted by noise ϵ for i times. This is equivalent to predicting the mean μ_θ of $p_\theta\left(\tau^{i-1} \mid \tau^i\right)$ as the function mapping from $\epsilon_\theta(\tau^i, i)$ to $\mu_\theta(\tau^i, i)$ is a closed-form expression.

4. Method

In this section, we first introduce the basic planning with the diffusion method and its limitations. Then, we propose AdaptDiffuser, a novel self-evolved sequence modeling method for decision-making with the basis of diffusion probabilistic models. AdaptDiffuser is designed to enhance the performance of diffusion models in existing decision-making tasks, especially the goal-conditioned tasks, and further improve their adaptability in unseen tasks without any expert data to supervise the training process.

4.1. Planning with Task-oriented Diffusion Model

Following previous work (Janner et al., 2022), we can re-define the planning trajectory as a special kind of sequence data with actions as an additional dimension of states like:

$$\boldsymbol{\tau} = \left[\begin{array}{cccc} \boldsymbol{s}_0 & \boldsymbol{s}_1 & ... & \boldsymbol{s}_T \\ \boldsymbol{a}_0 & \boldsymbol{a}_1 & ... & \boldsymbol{a}_T \end{array} \right] \qquad (6)$$

Then we can use the diffusion probabilistic model to perform trajectory generation. However, the aim of planning is not to restore the original trajectory but to predict future actions with the highest reward-to-go, the offline reinforcement learning should be formulated as a conditional generative problem with guided diffusion models that have achieved great success on image synthesis (Dhariwal & Nichol, 2021). So, we drive the conditional diffusion process:

$$q(\boldsymbol{\tau}^{i+1}|\boldsymbol{\tau}^i), \quad p_\theta(\boldsymbol{\tau}^{i-1}|\boldsymbol{\tau}^i, \boldsymbol{y}(\boldsymbol{\tau})) \qquad (7)$$

where the new term $\boldsymbol{y}(\boldsymbol{\tau})$ is some specific information of the given trajectory $\boldsymbol{\tau}$, such as the reward-to-go (return) $\mathcal{J}(\boldsymbol{\tau}^0)$ of the trajectory, the constraints that must be satisfied by the trajectory and so on. On this basis, we can rewrite the optimization objective as,

$$\theta^* = \arg\min_\theta -\mathbb{E}_{\boldsymbol{\tau}^0}\left[\log p_\theta(\boldsymbol{\tau}^0|\boldsymbol{y}(\boldsymbol{\tau}^0))\right] \qquad (8)$$

Therefore, for tasks aiming to maximize the reward-to-go, we take $\mathcal{O}_t$ to denote the optimality of the trajectory at timestep t. And $\mathcal{O}_t$ obeys Bernoulli distribution with $p(\mathcal{O}_t = 1) = \exp(\gamma^t \mathcal{R}(\boldsymbol{s}_t, \boldsymbol{a}_t))$. When $p(\mathcal{O}_{1:T} \mid \boldsymbol{\tau}^i)$ meets specific Lipschitz conditions, the conditional transition probability of the reverse diffusion process can be approximated as (Feller, 2015):

$$p_\theta(\boldsymbol{\tau}^{i-1} \mid \boldsymbol{\tau}^i, \mathcal{O}_{1:T}) \approx \mathcal{N}(\boldsymbol{\tau}^{i-1}; \mu_\theta + \alpha\Sigma g, \Sigma) \qquad (9)$$

where, $g = \nabla_{\boldsymbol{\tau}} \log p(\mathcal{O}_{1:T} \mid \boldsymbol{\tau})|_{\boldsymbol{\tau}=\mu_\theta}$

$$= \sum_{t=0}^T \gamma^t \nabla_{\boldsymbol{s}_t, \boldsymbol{a}_t} \mathcal{R}(\boldsymbol{s}_t, \boldsymbol{a}_t)|_{(\boldsymbol{s}_t, \boldsymbol{a}_t)=\mu_t} = \nabla_{\boldsymbol{\tau}} \mathcal{J}(\mu_\theta).$$

Besides, for tasks aiming to satisfy single point conditional constraint (e.g. goal conditioned tasks), the constraint can be
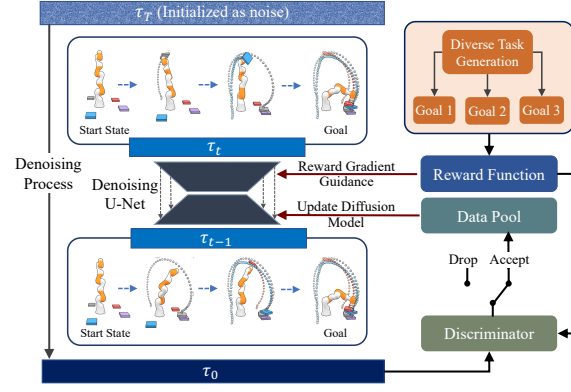

Figure 2. Overall framework of AdaptDiffuser. To improve the adaptability of the diffusion model to diverse tasks, rich data with distinct objectives is generated, guided by each task's reward function. During the diffusion denoising process, we utilize a pre-trained denoising U-Net to progressively generate high-quality trajectories. At each denoising time step, we take the task-specific reward of a trajectory to adjust the gradient of state and action sequence, thereby creating trajectories that align with specific task objectives. Subsequently, the generated synthetic trajectory is evaluated by a discriminator to see if it meets the standards. If yes, it is incorporated into a data pool to fine-tune the diffusion model. The procedure iteratively enhances the generalizability of our model for both seen and unseen settings.

simplified by substituting conditional values for the sampled values of all diffusion timesteps $i \in \{0, 1, ..., N\}$.

Although this paradigm has achieved competitive results with previous planning methods which are not based on diffusion models, it only performs conditional guidance during the reverse diffusion process and assumes the unconditional diffusion model is trained perfectly over the forward process. However, as depicted in Eq. 9, the quality of generated trajectory $\boldsymbol{\tau}$ depends not only on the guided gradient g but more on the learned means μ_θ and covariance Σ of the unconditional diffusion model. If the learned μ_θ deviates far from the optimal trajectory, no matter how strong the guidance g is, the final generated result will be highly biased and of low quality. Then, learning from Eq. 5, the quality of μ_θ hinges on the training data, the quality of which, however, is uneven across different tasks, especially on unseen tasks. Previous diffusion-based planning methods have not solved the problem which limits the performance of these methods on both existing and unseen tasks, and thus have poor adaptation ability.

4.2. Self-evolved Planning with Diffusion

Therefore, with the aim to improve the adaptation ability of these planners, we propose AdaptDiffuser which is a novel self-evolved decision-making approach based on diffusion probabilistic models, to enhance the quality of the trained means μ_θ and covariance Σ of the forward diffusion pro-

cess. AdaptDiffuser relies on self-evolved synthetic data generation to enrich the training dataset, denoted as $\boldsymbol{\tau}_0$, and fine-tuning on these synthetic data to boost performance. After that, AdaptDiffuser follows the paradigm depicted in Eq. 9 to find the optimal action sequence for a given task, based on the guidance of reward gradients.

As shown in Figure 2, to implement AdaptDiffuser, we firstly generate a large number of synthetic demonstration data for unseen tasks which do not exist in the training dataset but simulate a wide range of scenarios and behaviors that the diffusion model may encounter in the real world. This synthetic data is iteratively generated through the sampling process of the original diffusion probabilistic model θ_0^* with reward guidance, taking the advantage of its great generation ability. We will discuss the details of the synthetic data generation in Section 4.3 and here we just abbreviate it as a function $\mathcal{G}(\mu_\theta, \Sigma, \nabla_\tau \mathcal{J}(\mu_\theta))$.

Secondly, we use a discriminator $\mathcal{D}$, defined by reward guidance and dynamics consistency, to select high-quality data from the generated data pool. With the aim to measure the dynamics consistency of the action sequence $\boldsymbol{a} = [\boldsymbol{a}_0, \boldsymbol{a}_1, ..., \boldsymbol{a}_T]$ denoised by diffusion model (a part of the trajectory $\boldsymbol{\tau}$), we adopt a different way from previous sequence modeling approaches which predict the rewards $\mathcal{R}(\boldsymbol{s}, \boldsymbol{a})$ simultaneously with states and actions. Detailedly, we only take the state sequence $\boldsymbol{s} = [\boldsymbol{s}_0, \boldsymbol{s}_1, ..., \boldsymbol{s}_T]$ of the generated trajectory and then perform state tracking control employing a traditional controller so as to derive real executable actions, denoted as $\widetilde{\boldsymbol{a}}$. For example, for the Maze2D task, we use a PID controller (Åström & Hägglund, 2006). Then, if we let $\widetilde{\boldsymbol{s}}_0 = \boldsymbol{s}_0$, we have $\widetilde{\boldsymbol{a}}_t = \text{PID}(\widetilde{\boldsymbol{s}}_t, \boldsymbol{s}_{t+1})$, $\widetilde{\boldsymbol{s}}_{t+1} = \mathcal{T}(\widetilde{\boldsymbol{s}}_t, \widetilde{\boldsymbol{a}}_t)$. we first use the controller to calculate an executable action $\widetilde{\boldsymbol{a}}_t$, and then perform $\widetilde{\boldsymbol{a}}_t$ to obtain the revised next state $\widetilde{\boldsymbol{s}}_{t+1}$. After that, we use the updated state $\widetilde{\boldsymbol{s}}_{t+1}$ and the state $\boldsymbol{s}_{t+2}$ in the generated trajectory to proceed to the next round. Furthermore, we calculate the revised reward $\widetilde{\mathcal{R}}(\boldsymbol{s}, \boldsymbol{a}) = \mathcal{R}(\widetilde{\boldsymbol{s}}, \widetilde{\boldsymbol{a}})$ using the new actions $\widetilde{\boldsymbol{a}}$ and states $\widetilde{\boldsymbol{s}}$. By using the revised reward to perform high-quality data selection, we can equate the consideration of dynamics consistency to the consideration of reward guidance, leading to the formal unity of the two objectives of the discriminator.

Finally, the selected trajectories are added to the set of expert data as synthetic expert data, and are used to fine-tune the diffusion probabilistic model. We repeat this process multiple times in order to continually improve the model's performance and adapt it to new tasks, ultimately improving its generalization performance. So, it can be formulated as,

$$
\begin{aligned}
\theta_k^* &= \arg\min_\theta -\mathbb{E}_{\hat{\boldsymbol{\tau}}_k}\left[\log p_\theta(\hat{\boldsymbol{\tau}}_k | \boldsymbol{y}(\hat{\boldsymbol{\tau}}_k))\right] \\
\boldsymbol{\tau}_{k+1} &= \mathcal{G}\left(\mu_{\theta_k^*}, \Sigma, \nabla_\tau \mathcal{J}(\mu_{\theta_k^*})\right) \\
\hat{\boldsymbol{\tau}}_{k+1} &= [\hat{\boldsymbol{\tau}}_k, \mathcal{D}(\widetilde{\mathcal{R}}(\boldsymbol{\tau}_{k+1}))]
\end{aligned}
\tag{10}
$$

where $k \in \{0, 1, ...\}$ is the number of iteration rounds and the initial dataset $\hat{\boldsymbol{\tau}}_0 = \boldsymbol{\tau}_0$.

4.3. Reward-guided Synthetic Data Generation

To improve the performance and adaptability of the diffusion probabilistic model on unseen tasks, we need to generate synthetic trajectory data using the learned diffusion model at the current iteration. We achieve it by defining a series of tasks with different goals and reward functions.

Continuous Reward Function. For the tasks with continuous reward function, represented by MuJoCo (Todorov et al., 2012), we follow the settings that define a binary random variable indicating the optimality with probability mapped from a continuous value, to convert the reward maximization problem to a continuous optimization problem. We can easily take Eq. 9 to generate synthetic results.

Sparse Reward Function. The reward function of tasks as typified by a goal-conditioned problem like Maze2D is a unit step function $\mathcal{J}(\boldsymbol{\tau}) = \chi_{\boldsymbol{s}_g}(\boldsymbol{\tau})$ whose value is equal to 1 if and only if the generated trajectory contains the goal state $\boldsymbol{s}_g$. The gradient of this reward function is Dirac delta function (Zhang, 2021) which is not a classical function and cannot be adopted as guidance. However, if it is considered from the perspective of taking the limit, the constraint can be simplified as replacing all corresponding sampled values with constraints over the diffusion timesteps.

Combination. Many realistic tasks need these two sorts of reward functions simultaneously. For example, if there exists an auxiliary task in Maze2D environment that requires the planner to not only find a way from the start point to the goal point but also collect the gold coin in the maze. This task is more difficult and it's infeasible to add this constraint to the sparse reward term because there is no idea about which timestep the generated trajectory should pass the additional reward point (denoted as $\boldsymbol{s}_c$). As a solution, we propose to combine these two sorts of methods with an auxiliary reward guiding function to satisfy the constraints.

$$
\mathcal{J}(\boldsymbol{\tau}) = \sum_{t=0}^T ||\boldsymbol{s}_t - \boldsymbol{s}_c||_p
\tag{11}
$$

where p represents p-norm. Then, with Eq. 11 we plug it into Eq. 9 as the marginal probability density function and force the last state of the generated trajectory $\boldsymbol{\tau}^0$ to be $\boldsymbol{s}_c$. The generated trajectories that meet the desired criteria of the discriminator are added to the set of training data for the diffusion model learning as synthetic expert data. This process is repeated multiple times until a sufficient amount of synthetic data has been generated. By iteratively generating and selecting high-quality data based on the guidance of expected return and dynamics transition constraints, we can boost the performance and enhance the adaptability of the diffusion probabilistic model.

5. Experiment

5.1. Benchmarks

Maze2D: Maze2D (Fu et al., 2020) environment is a navigation task in which a 2D agent needs to traverse from a randomly designated location to a fixed goal location where a reward of 1 is given. No reward shaping is provided at any other location. The objective of this task is to evaluate the ability of offline RL algorithms to combine previously collected sub-trajectories in order to find the shortest path to the evaluation goal. Three maze layouts are available: "umaze", "medium", and "large". The expert data for this task is generated by selecting random goal locations and using a planner to generate sequences of waypoints that are followed using a PD controller to perform dynamic tracking.

MuJoCo: MuJoCo (Todorov et al., 2012) is a physics engine that allows for real-time simulation of complex mechanical systems. It has three typical tasks: Hopper, HalfCheetah, and Walker2d. Each task has 4 types of datasets to test the performance of an algorithm: "medium", "random", "medium-replay" and "medium-expert". The "medium" dataset is created by training a policy with a certain algorithm and collecting 1M samples. The "random" dataset is created by using a randomly initialized policy. The "medium-replay" dataset includes all samples recorded during training until the policy reaches a certain level of performance. There is also a "medium-expert" dataset which is a mix of expert demonstrations and sub-optimal data.

KUKA Robot: The KUKA Robot (Schreiber et al., 2010) benchmark is a standardized evaluation tool that is self-designed to measure the capabilities of a robot arm equipped with a suction cup at the end. It consists of two tasks: conditional stacking (Janner et al., 2022) and pick-and-place. More details can be seen in Sec. 5.3.2. By successfully completing these tasks, the KUKA Robot benchmark can accurately assess the performance of the robot arm and assist developers in improving its design.

5.2. Performance Enhancement on Existing Tasks

5.2.1. EXPERIMENTS ON MAZE2D ENVIRONMENT

Overall Performance. Navigation in Maze2D environment takes planners hundreds of steps to reach the goal location. Even the best model-free algorithms have to make great efforts to adequately perform credit assignments and reliably reach the target. We plan with AdaptDiffuser using the strategy of sparse reward function to condition on the start and goal location. We compare our method with the best model-free algorithms (IQL Kostrikov et al. 2021 and CQL Kumar et al. 2020), conventional trajectory optimizer MPPI (Williams et al., 2015) and previous diffusion-based approach Diffuser (Janner et al., 2022) in Table 1. This comparison is fair because model-free methods can also identify

Table 1. **Offline Reinforcement Learning Performance in Maze2d Environment.** We show the results of AdaptDiffuser and previous planning methods to validate the bootstrapping effect of our method on a goal-conditioned task.

Environment	MPPI	CQL	IQL	Diffuser	AdaptDiffuser
U-Maze	33.2	5.7	47.4	113.9	**135.1** ±5.8
Medium	10.2	5.0	34.9	121.5	**129.9** ±4.6
Large	5.1	12.5	58.6	123.0	**167.9** ±5.0
Average	16.2	7.7	47.0	119.5	**144.3**

(a) Diffuser   (b) AdaptDiffuser   (c) Diffuser (*Failed*)   (d) AdaptDiffuser
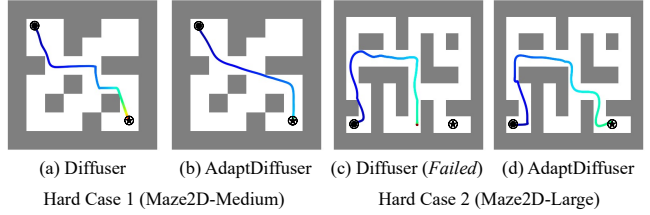
Hard Case 1 (Maze2D-Medium)   Hard Case 2 (Maze2D-Large)

Figure 3. **Hard Cases of Maze2D with Long Planning Path.** Paths are generated in the Maze2D environment with a specified start ◉ and goal ✪ condition.

the location of the goal point which is the only state with a non-zero reward.

As shown in Table 1, scores achieved by AdaptDiffuser are over 125 in all maze sizes and are 20 points higher than those of Diffuser in average, indicating our method's strong effectiveness in goal-conditioned tasks.

Visualization of Hard Cases. In order to more intuitively reflect the improvement of our method compared with previous Diffuser (Janner et al., 2022), we select one difficult planning example of Maze2D-Medium and one of Maze2D-Large respectively for visualization, as shown in Figure 3. Among the Maze2D planning paths with sparse rewards, the example with the longest path to be planned is the hardest one. Therefore, in Maze2D-Medium (Fig. 3 (a) (b)), we designate the start point as (1, 1) with goal point (6, 6), while in Maze2D-Large (Fig. 3 (c) (d)), we specify the start point as (1, 7) with goal point (9, 7) in the figure.

It can be observed from Fig. 3 that in Hard Case 1, AdaptDiffuser has generated a shorter and smoother path than that generated by Diffuser which achieves a larger reward. And in Hard Case 2, previous Diffuser method even fails to plan while our AdaptDiffuser derives a feasible path.

5.2.2. EXPERIMENTS ON MUJOCO ENVIRONMENT

MuJoCo tasks are employed to test the performance enhancement of our AdaptDiffuser learned from heterogeneous data of varying quality using the publicly available D4RL datasets (Fu et al., 2020). We evaluate our approach with a number of existing algorithms that cover a variety of data-driven methodologies, including model-free RL algorithms like CQL (Kumar et al., 2020) and IQL

Table 2. **Offline Reinforcement Learning Performance in MuJoCo Environment.** We report normalized average returns of D4RL tasks (Fu et al., 2020) in the table. And the mean and the standard error are calculated over 3 random seeds.

Dataset	Environment	BC	CQL	IQL	DT	TT	MOPO	MOReL	MBOP	Diffuser	AdaptDiffuser
Med-Expert	HalfCheetah	55.2	91.6	86.7	86.8	95.0	63.3	53.3	**105.9**	88.9	89.6 ±0.8
Med-Expert	Hopper	52.5	105.4	91.5	107.6	**110.0**	23.7	108.7	55.1	103.3	**111.6** ±2.0
Med-Expert	Walker2d	**107.5**	108.8	109.6	108.1	101.9	44.6	95.6	70.2	106.9	**108.2** ±0.8
Medium	HalfCheetah	42.6	44.0	**47.4**	42.6	**46.9**	42.3	42.1	44.6	42.8	44.2 ±0.6
Medium	Hopper	52.9	58.5	66.3	67.6	61.1	28.0	95.4	48.8	74.3	**96.6** ±2.7
Medium	Walker2d	75.3	72.5	78.3	74.0	79.0	17.8	77.8	41.0	79.6	**84.4** ±2.6
Med-Replay	HalfCheetah	36.6	**45.5**	**44.2**	36.6	41.9	53.1	40.2	42.3	37.7	38.3 ±0.9
Med-Replay	Hopper	18.1	95.0	94.7	82.7	91.5	67.5	**93.6**	12.4	**93.6**	92.2 ±1.5
Med-Replay	Walker2d	26.0	77.2	73.9	66.6	82.6	39.0	49.8	9.7	70.6	**84.7** ±3.1
Average		51.9	77.6	77.0	74.7	78.9	42.1	72.9	47.8	77.5	**83.4**

(Kostrikov et al., 2021); return-conditioning approaches like Decision Transformer (DT) (Chen et al., 2021a); and model-based RL algorithms like Trajectory Transformer (TT) (Janner et al., 2021), MOPO (Yu et al., 2020), MOReL (Kidambi et al., 2020), and MBOP (Argenson & Dulac-Arnold, 2020). The results are shown in Table 2. Besides, it is also worth noting that in the MuJoCo environment, the state sequence $\widetilde{s}$ derived by taking the generated actions a is very close to the generated state sequence s, so we directly use $\widetilde{\mathcal{R}}(s, a) = \mathcal{R}(s, a)$ in this dataset.

Observed from the table, our method AdaptDiffuser is either competitive or outperforms most of the offline RL baselines across all three different locomotion settings. And more importantly, compared with Diffuser (Janner et al., 2022), our method achieves higher reward in almost all the datasets and improves the performance greatly, especially in "Hopper-Medium" and "Walker2d-Medium" environments. We analyze that this is because the quality of the original data in the "Medium dataset" is poor, so AdaptDiffuser has an evident effect on improving the quality of the training dataset, thus significantly enhancing the performance of the planner based on the diffusion probabilistic model. The results of the "Medium-Expert" dataset verify this analysis because the quality of original data in the "Medium-Expert" dataset (especially the Halfcheetah environment) has been good enough, making the generation of new data only has a little gain on the model performance.

5.3. Adaptation Ability on Unseen Tasks

5.3.1. MAZE2D WITH GOLD COIN PICKING TASK

On top of existing Maze2D settings, we carefully design a new task that requires the agent to navigate as well as pick all gold coins in the maze. We show an example with an additional reward on (4, 2) in Figure 4. We can see that when there is no additional reward, both Diffuser (Janner et al., 2022) and our method AdaptDiffuser choose the shorter path at the bottom of the maze to reach the goal point. And then, when there are additional rewards in the (4, 2) position, both
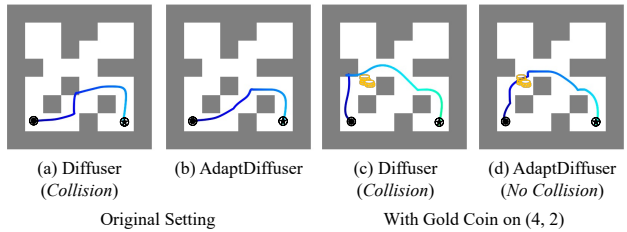

(a) Diffuser   (b) AdaptDiffuser   (c) Diffuser   (d) AdaptDiffuser
(*Collision*)   (*Collision*)   (*No Collision*)

Original Setting   With Gold Coin on (4, 2)

Figure 4. **Maze2d Navigation with Gold Coin Picking Task.** Subfigures (a) (b) is the original setting to navigate from the specified start ◉ to the goal ★. Subfigures (c) (d) add additional reward 🪙 and require planner to find a path picking all gold coins.

planners change to the path in the middle of the maze under the guidance of rewards. However, at this time, the path generated by Diffuser causes the agent to collide with the wall, while AdaptDiffuser generates a smoother collision-free path, reflecting the superiority of our method.

5.3.2. KUKA PICK AND PLACE TASK

Task Specification. There are two tasks in the KUKA robot arm environment. One is the conditional stacking task, as defined in (Janner et al., 2022), where the robot must correctly stack blocks in a predetermined order on a designated location, using blocks that have been randomly placed. And the other is the pick-and-place task designed by us, which aims to place the randomly initialized blocks in their own target locations in a predetermined order. The reward functions of both tasks are defined as one upon successful placements and zero otherwise.

To test the adaptation capability of AdaptDiffuser and other baselines, we only provide expert trajectory data for the conditional stacking task, which is generated by PDDLStream (Garrett et al., 2020), but we require the planner to generalize to pick-and-put task without any expert data. The performance of the pick-and-place task is supposed to be a good measure of the planner's adaptability.

Adaptation Performance. In KUKA pick-and-place task, we define the guidance of the conditional diffusion model

Table 3. **Adaptation Performance on Pick-and-Place Task**

Environment	Diffuser	AdaptDiffuser
Pick and Place setup 1	28.16 ±2.0	**36.03** ±2.1
Pick and Place setup 2	35.25 ±1.4	**39.00** ±1.3
Average	31.71	**37.52**

(a) Start   (b) Place Block 1   (c) Place Block 2
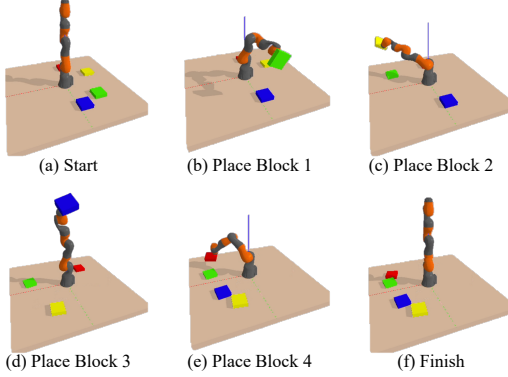
(d) Place Block 3   (e) Place Block 4   (f) Finish

Figure 5. **Visualization of KUKA Pick-and-Place Task.** We require the KUKA Arm to move the blocks from their random initialized positions on the right side of the table to the left and arrange them in the order of yellow, blue, green, and red (from near to far).

as the gradient of the reward function about the distance between the current location and the target location. Then, the adaptation performance is displayed in Table 3. There are two setups in KUKA benchmark. In setup 1, the four blocks are initialized randomly on the floor, while in setup 2, the four blocks are stacked at a random location at the beginning. As shown in Table 3, AdaptDiffuser outperforms Diffuser greatly on both setups while achieving higher performance at setup 2 because all of the blocks start from the same horizontal position. We visualize a successful case of the KUKA pick-and-place task in Figure 5, and more visualization results can be seen in Appendix B.

5.4. Ablation Study

5.4.1. ABLATION ON ITERATIVE STEPS

In order to verify the lifting effect of iterative data generation of our method AdaptDiffuser to improve the performance of the planner, we conduct an ablation experiment on the number of iterative steps of AdaptDiffuser in the MuJoCo environment of D4RL.

As shown in Table 4, with "Medium" dataset, due to the low quality of the original dataset, although the data generated in the first step has greatly supplemented the training dataset and greatly improved the performance (referring to Sec 5.2.2), the performance achieved after the second step is still significantly improved compared with that of the first step. However, for "Medium-Expert" dataset, because the expert data of the dataset has covered most of the environment, and the newly generated data is only more suitable for the

Table 4. **Ablation on Iterative Steps.** The mean and the standard error are calculated over 3 random seeds.

Dataset	Environment	1st Step	2nd Step
Medium-Expert	HalfCheetah	**89.3** ±0.6	89.6 ±0.8
Medium-Expert	Hopper	**110.7** ±3.2	111.6 ±2.0
Medium-Expert	Walker2d	**107.7** ±0.9	108.2 ±0.8
Medium	HalfCheetah	43.8 ±0.5	44.2 ±0.6
Medium	Hopper	95.4 ±3.4	**96.6** ±2.7
Medium	Walker2d	83.2 ±3.5	**84.4** ±2.6
Average		88.4	**89.1**

Table 5. **Ablation study on different amounts of expert data.**

	20% $\mathcal{D}$	50% $\mathcal{D}$	100% $\mathcal{D}$
Diffuser	105.0	107.9	123.0
AdaptDiffuser	**112.5**	**123.8**	**167.9**

planner to learn. So, after a certain improvement in the first step, the subsequent growth is not obvious. The above experiments verify the effectiveness of AdaptDiffuser for the multi-step iterative paradigm, and also show that the boosting effect is no longer obvious after the algorithm performance reaches a certain level.

5.4.2. ABLATION ON INSUFFICIENT DATA & TRAINING

To demonstrate the superiority of our method over previous diffusion-based work Diffuser (Janner et al., 2022) when the expert data is limited and the training is insufficient, we conducted experiments on the Maze2d-Large dataset using different percentages of expert data (e.g. 20%, 50%) with only 25% training steps to train our model. The results are shown in Table 5. The setting 100%$\mathcal{D}$ denotes the full training setting. We can see our AdaptDiffuser, which uses only 50% data and 25% training steps, beats the fully trained Diffuser. AdaptDiffuser can achieve good performance with a small amount of expert data and training steps.

6. Conclusion

We present AdaptDiffuser, a method for improving the performance of diffusion-based planners in offline reinforcement learning through self-evolution. By generating synthetic expert data using a diffusion model and filtering out high-quality data using a reward-guided discriminator, AdaptDiffuser is able to enhance the performance of diffusion models in existing decision-making tasks, especially the goal-conditioned tasks, and further improve the adaptability in unseen tasks without any expert data. Our experiments on two widely-used offline RL benchmarks and our carefully designed unseen tasks in KUKA and Maze2d environments validate the effectiveness of AdaptDiffuser.

Future works. Future studies could concentrate on improving the sampling speed and investigating challenges in the face of high-dimensional input tasks.

References

Agarwal, R., Schuurmans, D., and Norouzi, M. An optimistic perspective on offline reinforcement learning. In *International Conference on Machine Learning*, pp. 104–114. PMLR, 2020.

Ajay, A., Du, Y., Gupta, A., Tenenbaum, J., Jaakkola, T., and Agrawal, P. Is conditional generative modeling all you need for decision-making? *arXiv preprint arXiv:2211.15657*, 2022.

Argenson, A. and Dulac-Arnold, G. Model-based offline planning. *arXiv preprint arXiv:2008.05556*, 2020.

Åström, K. J. and Hägglund, T. Pid control. *IEEE Control Systems Magazine*, 1066, 2006.

Austin, J., Johnson, D. D., Ho, J., Tarlow, D., and van den Berg, R. Structured denoising diffusion models in discrete state-spaces. In *Advances in Neural Information Processing Systems*, 2021.

Buckman, J., Gelada, C., and Bellemare, M. G. The importance of pessimism in fixed-dataset policy optimization. *arXiv preprint arXiv:2009.06799*, 2020.

Chen, L., Lu, K., Rajeswaran, A., Lee, K., Grover, A., Laskin, M., Abbeel, P., Srinivas, A., and Mordatch, I. Decision transformer: Reinforcement learning via sequence modeling. *Advances in neural information processing systems*, 34:15084–15097, 2021a.

Chen, N., Zhang, Y., Zen, H., Weiss, R. J., Norouzi, M., and Chan, W. Wavegrad: Estimating gradients for waveform generation. In *International Conference on Learning Representations*, 2021b.

Dhariwal, P. and Nichol, A. Q. Diffusion models beat GANs on image synthesis. In *Advances in Neural Information Processing Systems*, 2021.

Du, Y. and Mordatch, I. Implicit generation and generalization in energy-based models. In *Advances in Neural Information Processing Systems*, 2019.

Du, Y., Li, S., and Mordatch, I. Compositional visual generation with energy based models. In *Advances in Neural Information Processing Systems*, 2020.

Feller, W. On the theory of stochastic processes, with particular reference to applications. In *Selected Papers I*, pp. 769–798. Springer, 2015.

Fu, J., Kumar, A., Nachum, O., Tucker, G., and Levine, S. D4rl: Datasets for deep data-driven reinforcement learning. *arXiv preprint arXiv:2004.07219*, 2020.

Garrett, C. R., Lozano-Pérez, T., and Kaelbling, L. P. Pddl-stream: Integrating symbolic planners and blackbox samplers via optimistic adaptive planning. In *Proceedings of the International Conference on Automated Planning and Scheduling*, volume 30, pp. 440–448, 2020.

Grathwohl, W., Wang, K.-C., Jacobsen, J.-H., Duvenaud, D., and Zemel, R. Learning the stein discrepancy for training and evaluating energy-based models without sampling. In *International Conference on Machine Learning*, 2020.

Ho, J., Jain, A., and Abbeel, P. Denoising diffusion probabilistic models. *Advances in Neural Information Processing Systems*, 33:6840–6851, 2020.

Hyvärinen, A. Estimation of non-normalized statistical models by score matching. *Journal of Machine Learning Research*, 2005.

Janner, M., Li, Q., and Levine, S. Offline reinforcement learning as one big sequence modeling problem. *Advances in neural information processing systems*, 34:1273–1286, 2021.

Janner, M., Du, Y., Tenenbaum, J. B., and Levine, S. Planning with diffusion for flexible behavior synthesis. *arXiv preprint arXiv:2205.09991*, 2022.

Kidambi, R., Rajeswaran, A., Netrapalli, P., and Joachims, T. Morel: Model-based offline reinforcement learning. *Advances in neural information processing systems*, 33:21810–21823, 2020.

Kingma, D. P. and Ba, J. Adam: A method for stochastic optimization. *arXiv preprint arXiv:1412.6980*, 2014.

Kostrikov, I., Nair, A., and Levine, S. Offline reinforcement learning with implicit q-learning. *arXiv preprint arXiv:2110.06169*, 2021.

Kumar, A., Zhou, A., Tucker, G., and Levine, S. Conservative q-learning for offline reinforcement learning. *Advances in Neural Information Processing Systems*, 33:1179–1191, 2020.

LeCun, Y., Chopra, S., Hadsell, R., Huang, F. J., and et al. A tutorial on energy-based learning. In *Predicting Structured Data*. MIT Press, 2006.

Levine, S., Kumar, A., Tucker, G., and Fu, J. Offline reinforcement learning: Tutorial, review, and perspectives on open problems. *arXiv preprint arXiv:2005.01643*, 2020.

Misra, D. Mish: A self regularized non-monotonic activation function. *arXiv preprint arXiv:1908.08681*, 2019.

Nijkamp, E., Hill, M., Zhu, S.-C., and Wu, Y. N. Learning non-convergent non-persistent short-run MCMC toward energy-based model. In *Advances in Neural Information Processing Systems*, 2019.

Prudencio, R. F., Maximo, M. R., and Colombini, E. L. A survey on offline reinforcement learning: Taxonomy, review, and open problems. *arXiv preprint arXiv:2203.01387*, 2022.

Ramesh, A., Dhariwal, P., Nichol, A., Chu, C., and Chen, M. Hierarchical text-conditional image generation with clip latents. *arXiv preprint arXiv:2204.06125*, 2022.

Rombach, R., Blattmann, A., Lorenz, D., Esser, P., and Ommer, B. High-resolution image synthesis with latent diffusion models. In *Proceedings of the IEEE/CVF Conference on Computer Vision and Pattern Recognition*, pp. 10684–10695, 2022.

Ronneberger, O., Fischer, P., and Brox, T. U-net: Convolutional networks for biomedical image segmentation. In *Medical Image Computing and Computer-Assisted Intervention–MICCAI 2015: 18th International Conference, Munich, Germany, October 5-9, 2015, Proceedings, Part III 18*, pp. 234–241. Springer, 2015.

Schreiber, G., Stemmer, A., and Bischoff, R. The fast research interface for the kuka lightweight robot. In *IEEE workshop on innovative robot control architectures for demanding (Research) applications how to modify and enhance commercial controllers (ICRA 2010)*, pp. 15–21. Citeseer, 2010.

Siegel, N. Y., Springenberg, J. T., Berkenkamp, F., Abdolmaleki, A., Neunert, M., Lampe, T., Hafner, R., Heess, N., and Riedmiller, M. Keep doing what worked: Behavioral modelling priors for offline reinforcement learning. *arXiv preprint arXiv:2002.08396*, 2020.

Sohl-Dickstein, J., Weiss, E., Maheswaranathan, N., and Ganguli, S. Deep unsupervised learning using nonequilibrium thermodynamics. In *International Conference on Machine Learning*, pp. 2256–2265. PMLR, 2015.

Song, J., Meng, C., and Ermon, S. Denoising diffusion implicit models. In *International Conference on Learning Representations*, 2021.

Song, Y. and Ermon, S. Generative modeling by estimating gradients of the data distribution. In *Advances in Neural Information Processing Systems*, 2019.

Sutton, R. S. Learning to predict by the methods of temporal differences. *Machine learning*, 3(1):9–44, 1988.

Sutton, R. S. and Barto, A. G. *Reinforcement learning: An introduction*. MIT press, 2018.

Todorov, E., Erez, T., and Tassa, Y. Mujoco: A physics engine for model-based control. In *2012 IEEE/RSJ international conference on intelligent robots and systems*, pp. 5026–5033. IEEE, 2012.

Wang, K., Zhao, H., Luo, X., Ren, K., Zhang, W., and Li, D. Bootstrapped transformer for offline reinforcement learning. *arXiv preprint arXiv:2206.08569*, 2022a.

Wang, Z., Hunt, J. J., and Zhou, M. Diffusion policies as an expressive policy class for offline reinforcement learning. *arXiv preprint arXiv:2208.06193*, 2022b.

Williams, G., Aldrich, A., and Theodorou, E. Model predictive path integral control using covariance variable importance sampling. *arXiv preprint arXiv:1509.01149*, 2015.

Wu, Y. and He, K. Group normalization. In *Proceedings of the European conference on computer vision (ECCV)*, pp. 3–19, 2018.

Wu, Y., Tucker, G., and Nachum, O. Behavior regularized offline reinforcement learning. *arXiv preprint arXiv:1911.11361*, 2019.

Yang, S., Wang, Z., Zheng, H., Feng, Y., and Zhou, M. A regularized implicit policy for offline reinforcement learning. *arXiv preprint arXiv:2202.09673*, 2022.

Yu, T., Thomas, G., Yu, L., Ermon, S., Zou, J. Y., Levine, S., Finn, C., and Ma, T. Mopo: Model-based offline policy optimization. *Advances in Neural Information Processing Systems*, 33:14129–14142, 2020.

Zhang, L. Dirac delta function of matrix argument. *International Journal of Theoretical Physics*, 60(7):2445–2472, 2021.

Zhou, L., Du, Y., and Wu, J. 3D shape generation and completion through point-voxel diffusion. In *International Conference on Computer Vision*, 2021.

A. Classifier-Guided Diffusion Model for Planning

In this section, we introduce theoretical analysis of conditional diffusion model in detail. We start with an unconditional diffusion probabilistic model with a standard reverse process as $p_\theta(\tau^i | \tau^{i+1})$. Then, with a specific label y (for example, goal point in Maze2D or specific reward function in MuJoCo) which is to be conditioned on given a noised trajectory τ^i, the reverse diffusion process can be redefined as $p_{\theta,\phi}(\tau^i | \tau^{i+1}, y)$. Apart from the parameters θ of original diffusion model, a new parameter ϕ is introduced here which describes the probability transfer model from noisy trajectory τ^i to the specific label y which is denoted as $p_\phi(y \mid \tau^i)$.

Lemma 1. The marginal probability of a conditional Markov's noising process q conditioned on y is equal to the marginal probability of the unconditional noising process.

$$q\left(\tau^{i+1} \mid \tau^i\right) = q\left(\tau^{i+1} \mid \tau^i, y\right) \tag{12}$$

Proof.

$$
\begin{aligned}
q\left(\tau^{i+1} \mid \tau^i\right) &= \int_y q\left(\tau^{i+1}, y \mid \tau^i\right) dy \\
&= \int_y q\left(\tau^{i+1} \mid \tau^i, y\right) p_\phi\left(y \mid \tau^i\right) dy \\
&= q\left(\tau^{i+1} \mid \tau^i, y\right) \int_y p_\phi\left(y \mid \tau^i\right) dy \\
&= q\left(\tau^{i+1} \mid \tau^i, y\right)
\end{aligned}
$$

The third equation holds because $q\left(\tau^{i+1} \mid \tau^i, y\right)$ fits another y-independent transition probability according to its definition.

Lemma 2. The probability distribution of specific label y conditioned on τ^i does not depend on τ^{i+1}.

$$p_{\theta,\phi}\left(y \mid \tau^i, \tau^{i+1}\right) = p_\phi\left(y \mid \tau^i\right) \tag{13}$$

Proof.

$$
\begin{aligned}
p_{\theta,\phi}\left(y \mid \tau^i, \tau^{i+1}\right) &= q\left(\tau^{i+1} \mid \tau^i, y\right) \frac{p_\phi\left(y \mid \tau^i\right)}{q\left(\tau^{i+1} \mid \tau^i\right)} \\
&= q\left(\tau^{i+1} \mid \tau^i\right) \frac{p_\phi\left(y \mid \tau^i\right)}{q\left(\tau^{i+1} \mid \tau^i\right)} \\
&= p_\phi\left(y \mid \tau^i\right)
\end{aligned}
$$

Theorem 1. The conditional sampling $p_{\theta,\phi}(\tau^i | \tau^{i+1}, y)$ is proportional to unconditional transition probability $p_\theta(\tau^i | \tau^{i+1})$ multiplied by classified probability $p_\phi(\tau^i \mid y)$.

$$p_{\theta,\phi}(\tau^i | \tau^{i+1}, y) = Z p_\theta(\tau^i | \tau^{i+1}) p_\phi(y | \tau^i) \tag{14}$$

Proof.

With the knowledge of conditional probability and Bayes' theorem, we have,

$$
\begin{aligned}
p_{\theta,\phi}(\tau^i | \tau^{i+1}, y) &= \frac{p_{\theta,\phi}\left(\tau^i, \tau^{i+1}, y\right)}{p_{\theta,\phi}\left(\tau^{i+1}, y\right)} \\
&= \frac{p_{\theta,\phi}\left(\tau^i, \tau^{i+1}, y\right)}{p_\phi\left(y \mid \tau^{i+1}\right) p_\theta\left(\tau^{i+1}\right)} \\
&= \frac{p_\theta\left(\tau^i \mid \tau^{i+1}\right) p_{\theta,\phi}\left(y \mid \tau^i, \tau^{i+1}\right) p_\theta\left(\tau^{i+1}\right)}{p_\phi\left(y \mid \tau^{i+1}\right) p_\theta\left(\tau^{i+1}\right)} \\
&= \frac{p_\theta\left(\tau^i \mid \tau^{i+1}\right) p_{\theta,\phi}\left(y \mid \tau^i, \tau^{i+1}\right)}{p_\phi\left(y \mid \tau^{i+1}\right)} \\
&= \frac{p_\theta\left(\tau^i \mid \tau^{i+1}\right) p_\phi\left(y \mid \tau^i\right)}{p_\phi\left(y \mid \tau^{i+1}\right)}
\end{aligned} \tag{15}
$$

The term $p_\phi\left(y \mid \tau^{i+1}\right)$ can be seen as a constant since it's not conditioned on τ^i at the diffusion timestep i. Proven.

Although exact sampling from this distribution (Equation 14) is difficult, (Sohl-Dickstein et al., 2015) demonstrates that it can be approximated as a modified Gaussian distribution. We show the derivation here.

On one hand, as Equation 4 shows, we can formulate the denoising process with a Gaussian distribution:

$$p_\theta(\tau^i \mid \tau^{i+1}) = \mathcal{N}(\mu, \Sigma) \tag{16}$$

$$\log p_\theta(\tau^i \mid \tau^{i+1}) = -\frac{1}{2}(\tau^i - \mu)^T \Sigma^{-1}(\tau^i - \mu) + C \tag{17}$$

And on the other hand, the number of diffusion steps are usually large, so the difference between τ^i and τ^{i+1} is small enough. We can apply Taylor expansion around $\tau^i = \mu$ to $\log p_\phi(y \mid \tau^i)$ as,

$$\log p_\phi\left(y \mid \tau^i\right) = \log p_\phi\left(y \mid \tau^i\right)\big|_{\tau^i=\mu} + \left(\tau^i - \mu\right) \nabla_{\tau^i} \log p_\phi\left(y \mid \tau^i\right)\big|_{\tau^i=\mu} \tag{18}$$

Therefore, synthesize Equation 17 and 18, we derive,

$$\begin{aligned}
\log p_{\theta,\phi}(\tau^i|\tau^{i+1}, y) &= \log p_\theta(\tau^i|\tau^{i+1}) + \log p_\phi(y|\tau^i) + C_1 \\
&= -\frac{1}{2}\left(\tau^i - \mu\right)^T \Sigma^{-1}\left(\tau^i - \mu\right) + \left(\tau^i - \mu\right) \nabla \log p_\phi\left(y \mid \tau^i\right) + C_2 \\
&= -\frac{1}{2}\left(\tau^i - \mu - \Sigma\nabla \log p_\phi\left(y \mid \tau^i\right)\right)^T \Sigma^{-1}\left(\tau^i - \mu - \Sigma\nabla \log p_\phi\left(y \mid \tau^i\right)\right) + C_3
\end{aligned} \tag{19}$$

which means,

$$p_{\theta,\phi}(\tau^i|\tau^{i+1}, y) \approx \mathcal{N}(\tau^i; \mu + \Sigma\nabla_\tau \log p_\phi\left(y \mid \tau^i\right), \Sigma) \tag{20}$$

And it's equal to Equation 9. Proven.

B. Visualization Results of KUKA Pick-and-Place Task

In this section, we show more visualization results about KUKA pick-and-place task. We require the KUKA Robot Arm to pick green, yellow, blue and red blocks with random initialized positions on the right side of the table one by one and move them to the left side in the order of yellow, blue, green and red (from near to far).
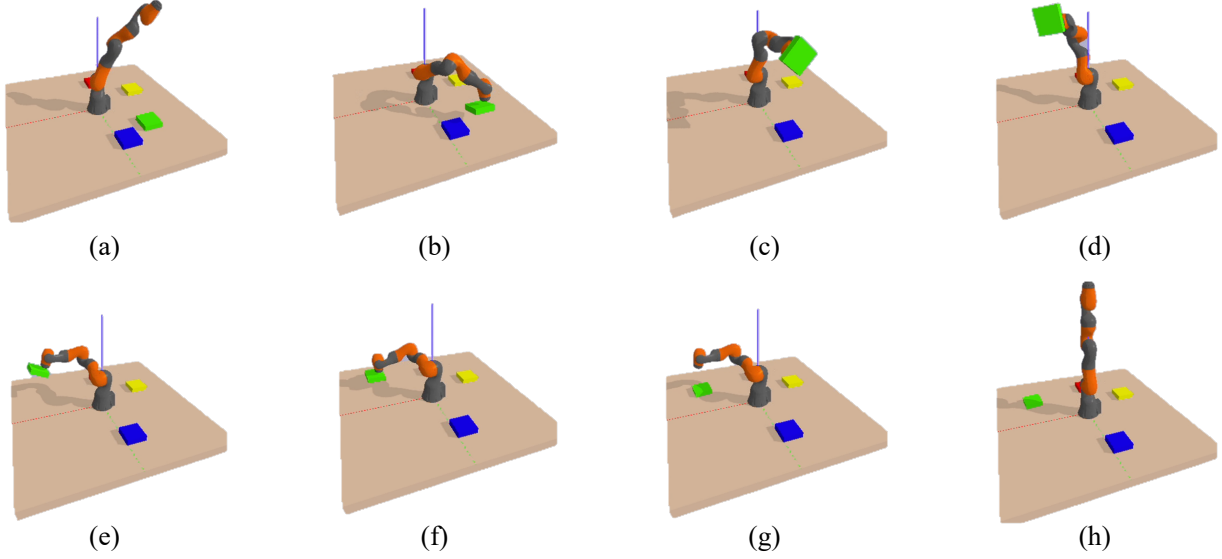
B.1. Pick and Place 1st Green Block

Figure 6. The Process of Pick and Place Block 1 (Green Block)
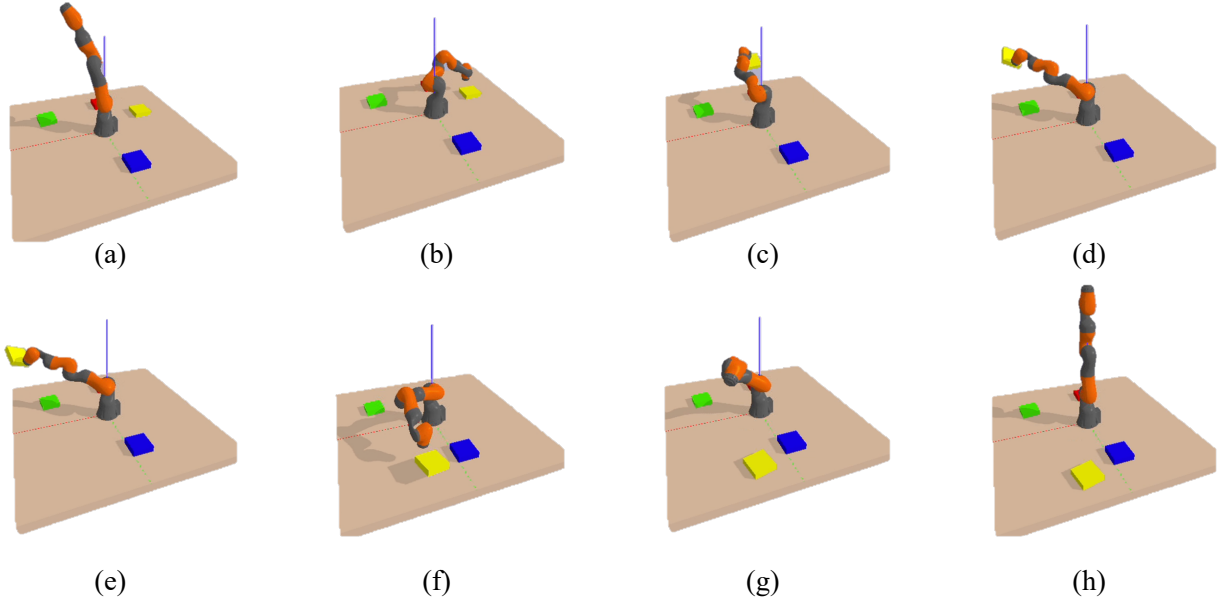
B.2. Pick and Place 2nd Yellow Block

Figure 7. The Process of Pick and Place Block 2 (Yellow Block)
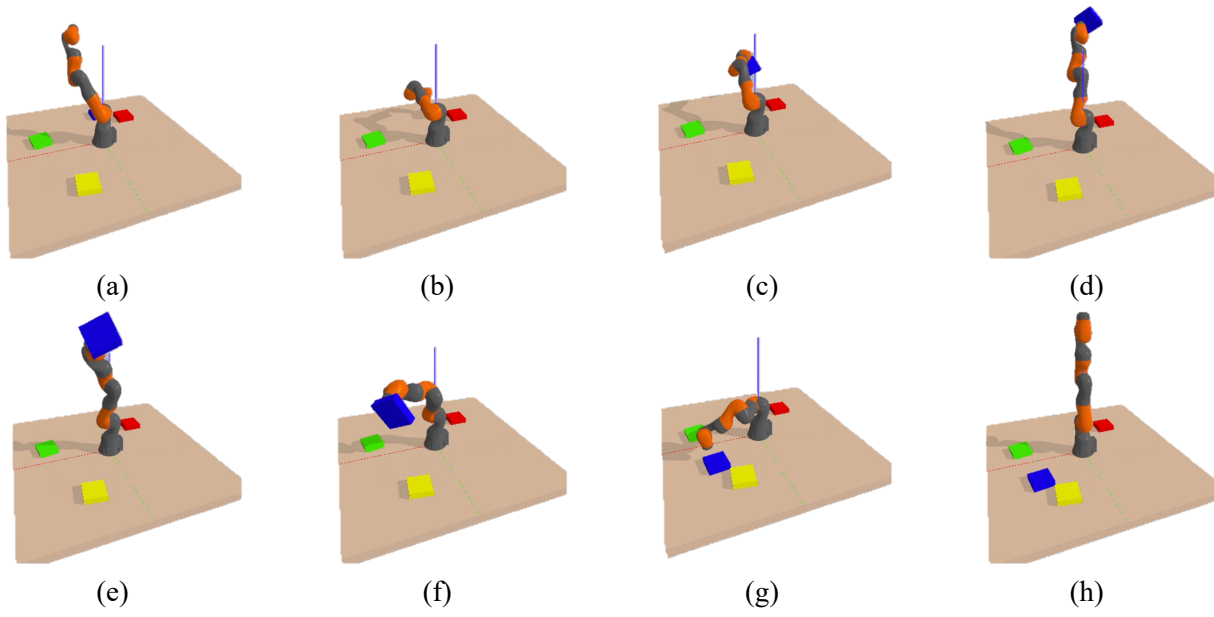
B.3. Pick and Place 3rd Blue Block

| | | | |
| (a) | (b) | (c) | (d) |

| | | | |
| (e) | (f) | (g) | (h) |

Figure 8. The Process of Pick and Place Block 3 (Blue Block)

B.4. Pick and Place 4th Red Block

| | | | |
| (a) | (b) | (c) | (d) |

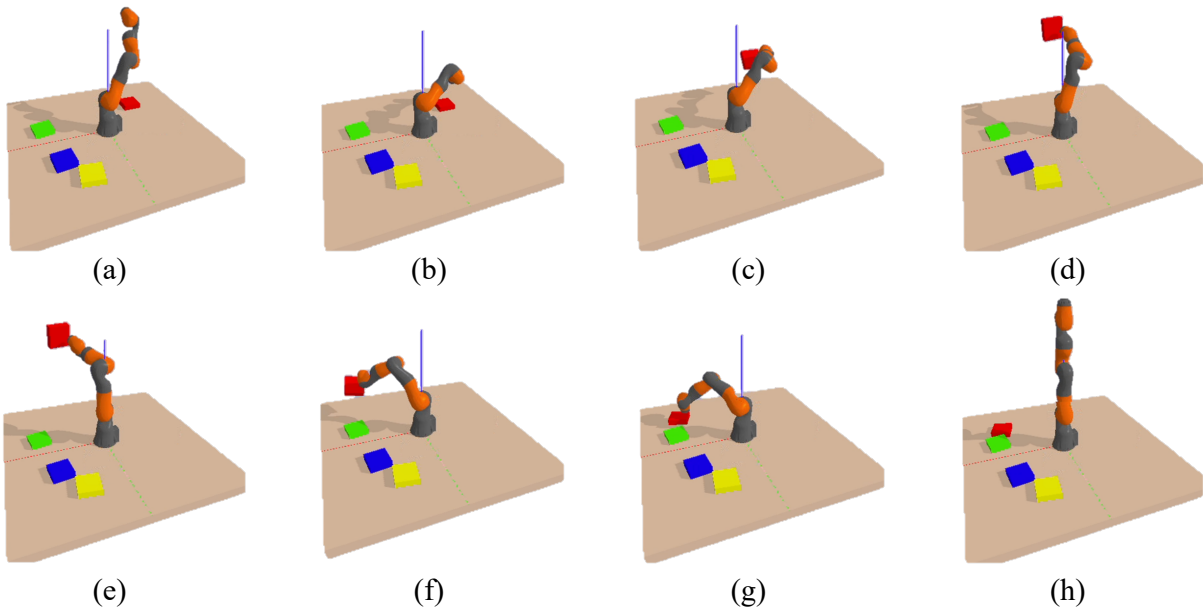| | | | |
| (e) | (f) | (g) | (h) |

Figure 9. The Process of Pick and Place Block 4 (Red Block)

C. Implementation Details and Hyperparameters

C.1. Details of Baseline Performances

Maze2D Tasks. We perform two different tasks on the Maze2D environment to validate the performance enhancement and adaptation ability of AdaptDiffuser on seen and unseen tasks.

- **Overall Performance of Navigation Task**: We report the performance of CQL and IQL on the standard Maze2D environments from Table 2 in D4RL whitepaper (Fu et al., 2020) and follow the hyperparameter settings described in (Janner et al., 2022). The performance of Diffuser also refers to Table 1 in (Janner et al., 2022). To reproduce the experimental results, we use the official implementation from the authors of IQL[1] and Diffuser[2].

- **Navigation with Gold Coin Picking Task**: We modified the official code of Diffuser and tuned over the hyperparameter $\alpha \in \{-50, -100, -200\}$ (the scalar of the guidance) in Equation 8 to adjust the planner to be competent for newly designed gold coin picking task, which is also the basis of our method AdaptDiffuser.

KUKA Pick and Place Tasks. Similar to the unseen tasks in Maze2D environment, we also ran the official implementation of IQL and Diffuser.

MuJoCo Locomotion Tasks. We report the scores of BC, CQL and IQL from Table 1 in (Kostrikov et al., 2021). We take down scores of DT from Table 2 in (Chen et al., 2021a), TT from Table 1 in (Janner et al., 2021), MOPO from Table 1 in (Yu et al., 2020), MOReL from Table 2 in (Kidambi et al., 2020), MBOP from Table 1 in (Argenson & Dulac-Arnold, 2020) and Diffuser from Table 2 in (Janner et al., 2022). All baselines are trained using the same offline dataset collected by a specific expert policy.

Table 6. **Metric Values for Reward Discriminator in MuJoCo Environment.** The rewards are calculated utilizing D4RL (Fu et al., 2020) locomotion suite.

Dataset	Environment	1st Step	2nd Step
Med-Expert	HalfCheetah	10840	10867
Med-Expert	Hopper	3639	3681
Med-Expert	Walker2d	4900	4950
Medium	HalfCheetah	5005	5150
Medium	Hopper	3211	3225
Medium	Walker2d	3700	3843
Med-Replay	HalfCheetah	4600	4800
Med-Replay	Hopper	3100	3136
Med-Replay	Walker2d	3900	3920

C.2. Metric Values for Reward Discriminator

Maze2D Environment. For the three different-size Maze2D settings, unlike MuJoCo, different trajectories are different in lengths which achieve different rewards. So, we not only consider the absolute value of the rewards $\mathcal{R}$ but also introduce trajectory length $\mathcal{L}$ and reward-length ratio into the criteria of discrimination. We prefer trajectories with longer lengths or those having higher reward-length ratios. Additionally, we denote the maximum episode steps of the environment as Max_e (Maze2D-UMaze: 300, Maze2D-Medium: 600, Maze2D-Large: 800). And then, we have following metrics to filter out high-quality data.

- **Maze2D-UMaze**: The trajectory is required to satisfy $\mathcal{L} > 200$ or $\mathcal{L} > 50$ and $\mathcal{R} + 1.0 * (Max_e - \mathcal{L}) > 210$ which is equal to measure the $\mathcal{R}/\mathcal{L}$.

- **Maze2D-Medium**: The trajectory is required to satisfy $\mathcal{L} > 450$ or $\mathcal{L} > 200$ and $\mathcal{R} + 1.0 * (Max_e - \mathcal{L}) > 400$.

- **Maze2D-Large**: The trajectory is required to satisfy $\mathcal{L} > 650$ or $\mathcal{L} > 270$ and $\mathcal{R} + 1.0 * (Max_e - \mathcal{L}) > 400$.

---

[1] https://github.com/ikostrikov/implicit_q_learning
[2] https://github.com/jannerm/diffuser

KUKA Robot Arm. For the KUKA Robot Arm environment, we define a sparse reward function that achieves one if and only if the placement is successful and zero otherwise. Therefore, we take the condition $\mathcal{R} >= 2.0$ which means at least half of the four placements are successful.

MuJoCo Environment. For MuJoCo locomotion environment, as we describe in Sec. 5.2.2, we directly use the reward derived after generated state sequence and action sequence to filter out high-quality synthetic data. The specific values for MuJoCo are shown in Table 6.

C.3. Amount of Synthetic Data for Each Iteration

The amount of synthetic data for each iteration is another important hyperparameter for AdaptDiffuser. Different tasks have different settings. We give detailed hyperparameters here.

Table 7. **Amount of Synthetic Data for Each Iteration.** The number of synthetic data for KUKA Arm pick-and place task consists of 1000 generated trajectories and 10000 cross-domain trajectories from the unconditional stacking task.

Dataset	Task	# of Expert Data	# of Synthetic Data
MuJoCo	Locomotion	$10^6, 2 \times 10^6$	50000
Maze2D	Navigation	$10^6, 2 \times 10^6, 4 \times 10^6$	10^6
Maze2D	Gold Coin Picking	0	10^6
KUKA Robot	Unconditional Stacking	10000	-
KUKA Robot	Pick-and-Place	0	11000

C.4. Other Details

1. A temporal U-Net (Ronneberger et al., 2015) with 6 repeated residual blocks is employed to model the noise ϵ_θ of the diffusion process. Each block is comprised of two temporal convolutions, each followed by group norm (Wu & He, 2018), and a final Mish non-linearity (Misra, 2019). Timestep embeddings are generated by a single fully-connected layer and added to the activation output after the first temporal convolution of each block.

2. The diffusion model is trained using the Adam optimizer (Kingma & Ba, 2014) with a learning rate of 2×10^{-4} and batch size of 32.

3. The training steps of the diffusion model are $1M$ for MuJoCo locomotion task, $2M$ for tasks on Maze2D and $0.7M$ for KUKA Robot Arm tasks.

4. The planning horizon T is set as 32 in all locomotion tasks, 128 for KUKA pick-and-place, 128 in Maze2D-UMaze, 192 in Maze2D-Medium, and 384 in Maze2D-Large.

5. We use $K = 100$ diffusion steps for all locomotion tasks, 1000 for KUKA robot arm tasks, 64 for Maze2D-UMaze, 128 for Maze2D-Medium, and 256 for Maze2D-Large.

6. We choose 2-norm as the auxiliary guided function in the combination setting of Section 4.3 and the guidance scale $\alpha \in \{1, 5, 10, 50, 100\}$ of which the exact choice depends on the specific task.